Available online at www.sciencedirect.com

ScienceDirect

Proceedings of the Combustion Institute 36 (2017) 2743–2751

Proceedings of the Combustion Institute

www.elsevier.com/locate/proci

Effects of temperature perturbation on direct detonation initiation

Chengken Qi, Zheng Chen*

SKLTCS, Department of Mechanics and Engineering Science, College of Engineering, Peking University, Beijing 100871, China

Received 4 December 2015; accepted 11 June 2016
Available online 21 June 2016

Abstract

Direct detonation initiation is simulated considering detailed chemistry for H_2/O_2/Ar mixture. The objective is to examine and interpret the effects of local temperature perturbation on direct detonation initiation. Temperature perturbations with different amplitudes are introduced in the region where the blast wave decays quickly. For the case without temperature perturbation, the supercritical, critical and subcritical regimes for direct detonation initiation are identified by continuously decreasing the initiation energy. The quasi-steady period in the critical case is investigated in details. The thermal states of flow particles at different initial locations within the quasi-steady region are tracked and analyzed; and the mechanism for the development of an over-driven detonation after the quasi-steady period is discussed. When a cold spot with large amplitude of temperature perturbation is introduced, the direct detonation initiation is prohibited, which is expected since low temperature in a cold spot greatly reduce the chemical reaction rate. However, it is observed unexpectedly that a cold spot with small amplitude of temperature perturbation can promote direct detonation initiation. Similarly, a hot spot with small amplitude of temperature perturbation inhibits direct detonation initiation; and it promotes direct detonation initiation when its amplitude is large enough. Such unexpected observation is caused by the opposite effects of temperature perturbation: local low temperature reduces the chemical reaction rate while it also increases the local volumetric energy density.

Keywords: Direct detonation initiation; Temperature perturbation; Cold spot; Hydrogen

1. Introduction

Understanding direct detonation initiation is important not only for fundamental combustion research but also for the development of high-performance detonation engines and the control of accidental explosion. During direct detonation initiation, detonation is instantaneously formed by the driven blast wave as a result of a large amount of energy deposition in an explosive gaseous mixture. According to experiments [1] and simulations [2], there are three regimes: supercritical, critical and subcritical, depending on whether the deposited energy is greater than, equal to, or less than a threshold value corresponding to

* Corresponding author.
E-mail addresses: cz@pku.edu.cn, chenzheng@coe.pku.edu.cn (Z. Chen).

http://dx.doi.org/10.1016/j.proci.2016.06.093
1540-7489 © 2016 by The Combustion Institute. Published by Elsevier Inc.

the critical energy E_C. In the supercritical regime with deposited energy being much larger than E_C, an overdriven detonation develops first and then it decays asymptotically approaching to the self-sustained Chapman–Jouguet (CJ) detonation. In the critical regime with deposited energy slightly above E_C, first the shock wave decays and the reaction front decouples from it, until a quasi-steady period during which the shock speed and reaction front propagation speed remain nearly constant. At the end of the quasi-steady period, local pressure pulse accumulates quickly and gets merged with the leading shock. Finally a detonation is formed. In the subcritical regime with the deposited energy below E_C, the shock speed continuously decreases and the reaction front decouples from the shock, which leads to detonation initiation failure.

In the literature, there are many studies on direct detonation initiation. Different models have been proposed to predict the critical energy of direct detonation initiation (e.g., [3] and references therein). For simplicity, one-step chemistry model was popularly used to analyze the direct detonation initiation process (e.g., [2, 4–7]). He and Clavin [2] found that the curvature effect can cause detonation initiation failure. Eckett et al. [6] showed that the unsteadiness effect also plays an important role in direct detonation initiation. However, as demonstrated by Mazaheri [8], one-step chemistry model cannot be used to predict a distinct value for the critical initiation energy below which no detonation occurs. Therefore, it was suggested [5,8] to use multi-step chemical model to study the critical energy of direct detonation initiation. For example, Ng and Lee [9] used three-step chain-branching chemical model to study the critical initiation energy and the influence of detonation instability on direct detonation initiation. Besides, to the authors' knowledge, only a few studies [10,11] used detailed chemistry to investigate the direct detonation initiation process.

Currently, the underlying mechanism for direct detonation initiation is still not well understood, especially for the quasi-steady period in critical initiation [5]. Besides, temperature inhomogeneity always exists due to various hydrodynamic fluctuations. The influence of temperature perturbation on direct detonation initiation has not been thoroughly examined. Chue et al. [12] studied the influence of periodic longitudinal perturbations on deflagration detonation transition. Mazaheri et al. [8] studied the effects of hot spot on direct detonation initiation using one-step chemistry and found that hot spot can promote detonation initiation. However, as mentioned before, one-step chemistry model has limitation in the study of direct detonation imitation. Besides, the influence of amplitude of temperature perturbation has not been thoroughly investigated previously.

Based on the above considerations, the objective of this work is to examine the effects of temperature perturbation on direct detonation initiation. One-dimensional (1D) simulations for direct detonation initiation in H_2/O_2/Ar mixture are conducted and detailed chemistry is employed. The details in direct detonation initiation is revealed. Besides, unlike previous studies, the influence of cold spot on direct detonation initiation is examined for the first time. Surprisingly, the cold spot is shown to be able to promote detonation initiation under certain conditions.

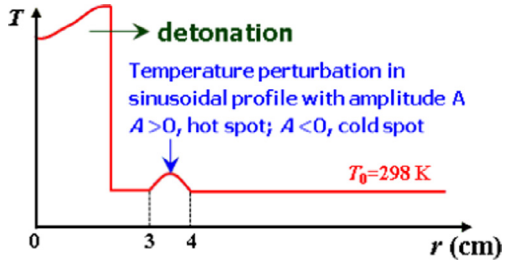

Fig. 1. Schematic of direct detonation initiation in premixture with temperature perturbation.

2. Numerical model and specifications

The numerical model is direct initiation of a 1D cylindrical detonation in H_2/O_2/Ar (the molar ratio is 2:1:7) mixture without/with temperature perturbation as sketched in Fig. 1. The initial temperature and pressure are fixed to be 298 K and 0.2 atm, respectively. As shown in Fig. 1, temperature perturbation in sinusoidal profile with amplitude of A and half-wavelength of 1 cm is introduced in the region of $3 \le r \le 4$ cm. Different amplitudes of temperature perturbation are investigated and both cold (i.e., $A<0$) and hot (i.e., $A>0$) spots are considered. Since the pressure is kept to be constant, the initial density in $3 \le r \le 4$ cm is different from that in the unperturbed region and it is determined from temperature based on equation of state for ideal gas.

In order to initiate the detonation, the ideal strong blast wave model governed by the similarity solution of Taylor [13] and Sedov [14] is used as the initial condition. The subsequent decay of the blast wave with chemical reaction is governed by Euler equations and simulated numerically. Similar approach was used in previous studies (e.g., [6,8,9]). The equivalent energy deposition is E_S and its unit is J/m since the cylindrical geometry is considered. The computational domain is $0 \le r \le 80$ cm. Zero flow speed and zero gradients of temperature and mass fractions are enforced at the center (r=0) and right boundary (r=80 cm).

The 1D direct detonation initiation process is simulated using the in-house code A-SURF [15–17]. The conservation equations for unsteady, 1D, compressible, multi-component,

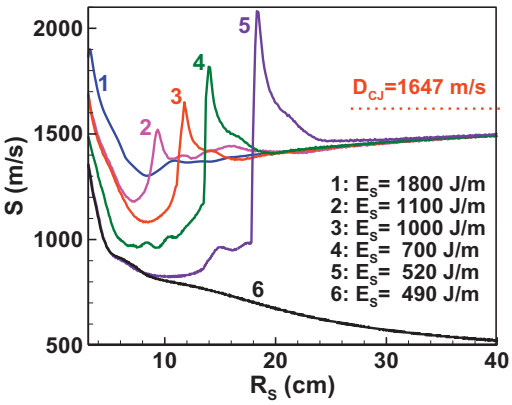

Fig. 2. Leading shock speed, S, as a function of its position, R_S, for different initiation energies. The C-J detonation speed is D_{CJ}=1647 m/s.

reactive flow in a cylindrical coordinate system are solved in A-SURF using the finite volume method. A-SURF has been successfully used in previous studies on flame propagation, end-gas autoignition and detonation development (e.g., [18–21]). The details on governing equations, numerical methods and code validations can be found in Refs. [15–17] and thereby are only provided in the Supplementary Document. Detailed hydrogen mechanism with 10 species and 21 elementary reactions [22] is considered in simulation. In order to efficiently resolve the reaction front, shock wave and detonation, dynamically adaptive mesh refinement strategy is adopted. The levels of refinement is 9 and the finest mesh size is 2 μm. The induction length is around 0.1 mm and it is covered by more than 30 points. As shown by Fig. S3 in the Supplementary Document, numerical convergence has been ensured by further decreasing the time step and mesh size in simulation.

3. Results and discussion

3.1. Cases without temperature perturbation (A=0)

We first consider direct detonation initiation in mixture without temperature perturbation (i.e., A=0). The results for different initiation energies covering three regimes (supercritical, critical and subcritical) are shown in Figs. 2–4. Figure 2 shows the change of leading shock speed with its position for different values of E_S. For reference, the CJ detonation speed of D_{CJ} =1647 m/s is shown as the horizontal dashed line. During direct detonation initiation, a strong blast wave is formed after the sudden deposition of initiation energy. For each initiation energy, the blast wave decays quickly at the very beginning. Therefore, Fig. 2 shows that there is a rapid decrease in the leading shock speed for R_S<5 cm. Figure 3 plots the temporal evolution of normalized pressure distributions for three initiation energies. The normalized pressure of von Neumann spike in CJ detonation, P_{VN}/P_0=27.2, is indicated by the horizontal dashed line.

At sufficient large initiation energy (E_S = 1800 J/m, see line #1 in Fig. 2 and case a in Fig. 3) above the critical value, the blast wave decays toward a self-sustained CJ detonation and this corresponds to the so-called supercritical case [1,2,9]. Line #1 in Fig. 2 indicates that the shock speed first decreases and then it increases approaching to the CJ detonation speed. Unlike the planar geometry [9], in the cylindrical geometry considered here the shock always first decays to some value below CJ speed even for very large value of E_S = 4000 J/m. The maximum pressure is also always below the pressure of von Neumann spike ($P<P_{VN}$, see lines #1–4 in Fig. 3a). This is due to the curvature effect as explained in [2,9]. For the supercritical case, rapid autoignition takes place behind the strong blast wave; and the reaction zone is intimately coupled and moves together with the leading shock wave. Figure 3(a) shows that the pressure decrease due to chemical heat release occurs just behind the shock wave-induced abrupt pressure rise. Similarly, the temperature profiles (not shown here due to space limit) also demonstrates that the reaction zone is closely coupled with the leading shock wave for the supercritical case.

When the initiation energy is below the critical energy (E_S=490 J/m<E_C, line #6 in Fig. 2 and case c in Fig. 3), the shock speed and peak pressure continuously decreases during its propagation. This corresponds to the subcritical case, in which the reaction zone fails to couple with the leading shock and the blast wave continues to decay to the sonic speed (line #6 in Fig. 2). The decoupling between the reaction zone and shock wave can be demonstrated by the temperature and pressure profiles. Lines #2 and #3 in Fig. 3(c) show that behind the abrupt pressure rise due to shock compression, there is a short plateau where the pressure remains nearly constant. After the plateau, heat release due to chemical reaction occurs and pressure decreases (similar plateau separating the shock wave and heat release zone is also observed in the temperature profiles). To further demonstrate the decoupling between the reaction zone and shock wave, we plot the trajectories of the shock wave and reaction front in Fig. 4. It is seen that for the subcritical case with E_S=490 J/m, the reaction front trajectory, OAB, always falls behind the shock wave trajectory OCD. Moreover, the distance between these two trajectories, OAB and OCD, increases with time. Therefore, the reaction front cannot couple with the shock wave and eventually detonation initiation fails in the subcritical case.

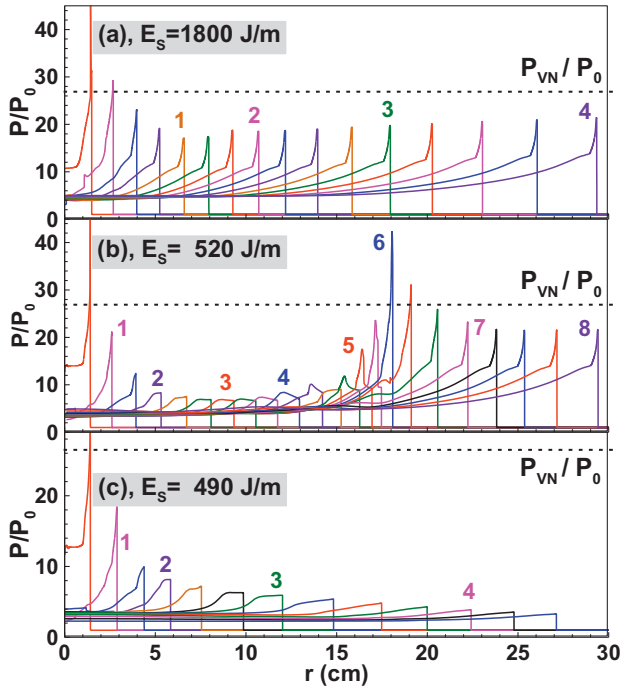

Fig. 3. Temporal evolution of normalized pressure distributions at three different initiation energies corresponding to (a) supercritical, (b) critical and (c) subcritical cases.

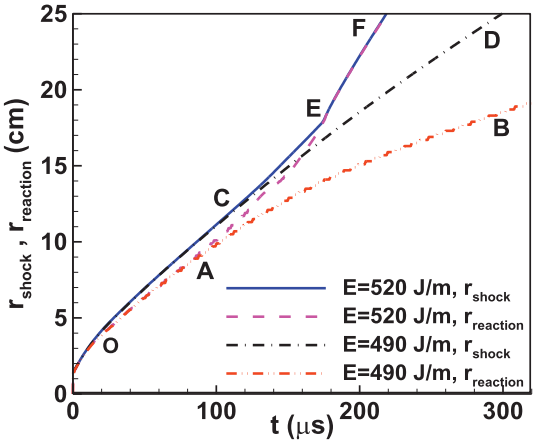

Fig. 4. Shock wave and reaction front trajectories for two initiation energies of 520 J/m (critical case) and 490 J/m (subcritical case).

When the initiation energy is slightly higher than the critical value (e.g., E_S=520 J/m>E_C, line #5 in Fig. 2 and case b in Fig. 3), the so-called critical regime is reached. The shock speed first decreases to a value around half D_{CJ} (line #5 in Fig. 2) and the reaction front starts to decouple with the leading shock (line #2 in Fig. 3b and point O in Fig. 4). Then the distance between these two fronts increases (lines #2 to #3 in Fig. 3b and points O to A in Fig. 4). After that, there is a period during which this distance keeps nearly constant and the leading shock and the reaction front propagate as a complex at nearly constant speed. It is referred to as the "quasi-steady" period [1,2,9]. At the end of the quasi-steady period, first a pressure pulse begins to develop near the reaction zone (line #4 in Fig. 3b). Then, the strength of the pressure pulse increases (lines #4 to #5 in Fig. 3b) and so does the

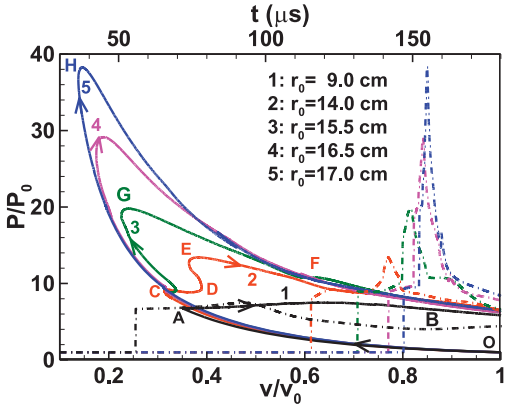

Fig. 5. The pressure versus specific volume, P–v, diagrams (solid lines) and pressure versus time (dashed lines) for particles at different initial position, r_0. The initiation energy is E_S=520 J/m (critical case).

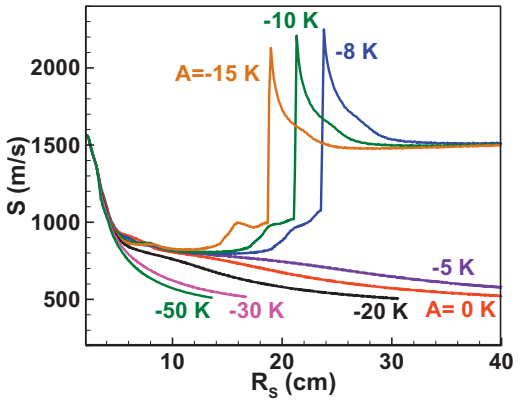

Fig. 6. Leading shock speed, S, as a function of its position, R_S, for different amplitude of temperature perturbations (A<0, cold spot). The initiation energy is fixed to be E_S=490 J/m, which corresponds to the subcritical case for A=0.

shock pressure. Finally, the shock wave accelerates abruptly and an overdriven detonation is developed (line #6 in Fig. 3b), which eventually decays to a self-sustained detonation (lines #7 to #8 in Fig. 3b). The onset of the overdriven detonation is caused by the pressure pulse generation and amplification near the reaction front [9]. The amplification of pressure pulse and the development of detonation is due to the coherent coupling between pressure pulse and chemical heat release, which can be explained by the SWACER mechanism [23,24] and shock-induced ignition [25,26].

To further reveal the chemical-gas dynamic interaction and combustion modes during the quasi-steady period, the thermal states of flow particles at different initial locations are tracked [27]: first, the position of a particle is updated by its current flow speed multiplying the time step size of 10^{-10} s; then, the thermal states of this particle are obtained from linear extrapolation of corresponding states at its two neighboring grids. We track the particles initially located at r_0=9–17 cm, covering the regions of quasi-steady period and the merging of the reaction front and the shock. Figure 5 shows the normalized pressure as a function of specific volume (solid lines). The associated times corresponding to pressure evolution are depicted by the dashed lines in Fig. 5. First, due to the passing of the leading shock, there is an adiabatic compression along the Hugoniot curve (OA or OC in Fig. 5) from the initial state at (P/P_0=1, v/v_0=1). For particle #1 initially at r_0=9 cm, the post-shock pressure (point A in Fig. 5) is relatively low and this particle experiences nearly constant-pressure combustion along AB. For particle #2, the post-shock pressure becomes higher; and it undergoes three stages: first, nearly constant-pressure combustion along CD; then, compression along DE; and finally, combustion and expansion along EF. For particle #3, the first stage of nearly constant-pressure combustion becomes much shorter than that of particle #2 and the compression stage becomes much stronger. Eventually for particles #4 and #5, these first two stages merge and a detonation develops. For particle #5, the pressure post-shock is much higher than P_{VN}, indicating the formation of an overdriven detonation.

In summary, three regimes for direct detonation initiation in H_2/O_2/Ar mixture, supercritical, critical and subcritical, are identified by decreasing the initiation energy. In the following subsection, the temperature perturbation is introduced and its influence on direct detonation initiation in the subcritical and critical regimes is examined.

3.2. Cases with temperature perturbation ($A \neq 0$)

In this study, both hot spot (A>0) and cold spot (A<0) are considered. As shown in Fig. 1, temperature perturbation is introduced in the region of $3 \le r \le 4$ cm. In this region, the rapid decay of the blast wave occurs (see Fig. 2). This is different from the previous study of Mazaheri [8] which considered hot spot in the region where quasi-steady propagation of shock-reaction front complex occurs.

Figure 6 demonstrates the influence of cold spot (A<0) on the leading shock speed. The initiation energy is fixed to be E_S=490 J/m, which corresponds to the subcritical case at A=0 (line #6 in Fig. 2). When the amplitude of temperature perturbation is A=−5 K, the shock speed is shown to be always larger than that for the unperturbed case of A=0, indicating that detonation initiation is enhanced even though detonation initiation still fails. When the amplitude of temperature perturbation is A=−8 K, successful detonation

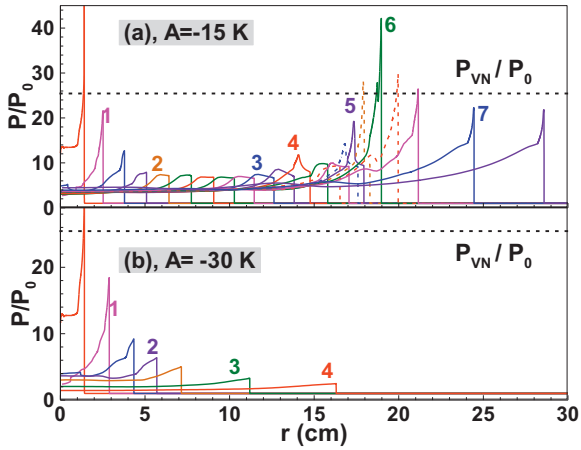

Fig. 7. Temporal evolution of normalized pressure distributions for (a) $A=-15$ K and (b) $A=-30$ K. The initiation energy is fixed to be $E_S=490$ J/m.

initiation is observed. The ran-up distance is shown to decrease as the amplitude of temperature perturbation is changed from $A=-8$ K to $A=-15$ K, indicating detonation initiation becomes easier at higher strength of the cold spot.

The temporal evolution of normalized pressure distributions for $A=-15$ K is shown in Fig. 7(a). It is seen that there is quasi-steady period during which the leading shock and reaction front propagates at nearly constant speed (lines #2 to #3 in Fig. 7a) and the quasi-steady period terminates with the abrupt formation of an over-driven detonation (lines #4 to #6 in Fig. 7a). This is similar to the results in Fig. 3(b) for the critical case with $E_S=520$ J/m and $A=0$. With further increase of the cold spot strength to $A=-20$ K, Fig. 6 shows that detonation initiation failure happens again. The shock speed is shown to become smaller at larger value of $|A|$ when $A<-20$ K. Figure 7(b) shows the temporal evolution of normalized pressure distributions for $A=-30$ K. The peak pressure is shown to continuously decrease, similar to the subcritical case of $E_S=490$ J/m and $A=0$ shown in Fig. 3(c).

Therefore, a cold spot with small amplitude of temperature perturbation promotes detonation initiation; and it inhibits detonation initiation when its amplitude is large enough. For the same initiation energy of $E_S=490$ J/m, we also consider the influence of a hot spot ($A>0$) and the results are shown in Fig. 8. When the amplitude of temperature perturbation increases from 0 K to 20 K, the shock decays faster and detonation initiation fails. However, successful detonation initiation is observed for $A=25$ K. With further increase of A from 25 K to 50 K, the ran-up distance becomes shorter and thereby detonation initiation becomes easier. Therefore, compared to the cold spot, the hot spot has the opposite influence on direct detonation initiation: a hot spot with small amplitude of temperature perturbation inhibits detonation initiation; and it promotes detonation initiation when its amplitude is large enough. Such trend was not observed in the previous study [8] which also investigated the influence of hot spot on direct detonation initiation.

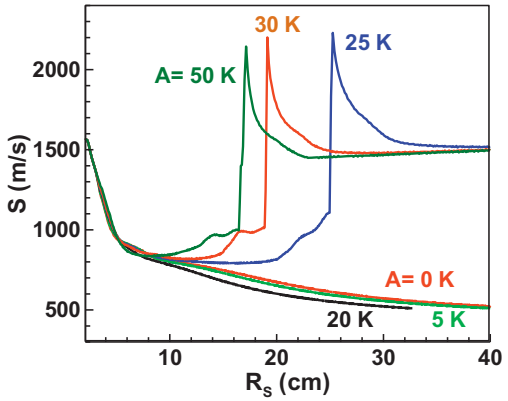

Fig. 8. Leading shock speed, S, as a function of its position, R_S, for different amplitude of temperature perturbations ($A>0$, hot spot). The initiation energy is fixed to be $E_S=490$ J/m.

Figure 9 summarizes the influence of different temperature perturbation (including both hot and cold spots) on the direct detonation imitation at the fixed value of $E_S=490$ J/m. In Fig. 9 we plot the shock speed at $R_S=15$ cm, which is somewhat arbitrarily chosen to characterize the initiation process. The shock speed is shown to change non-monotonically with the amplitude of temperature perturbation. The horizontal dashed line denotes the speed of S=790 m/s and it separates successful (closed symbols) and failed (open symbols)

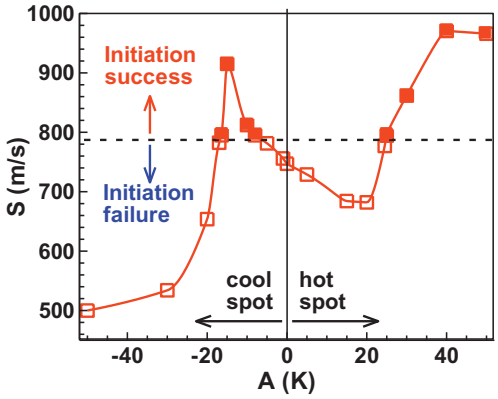

Fig. 9. Change of the shock speed at R_S=15 cm with the amplitude of temperature perturbation. The initiation energy is fixed to be E_S=490 J/m.

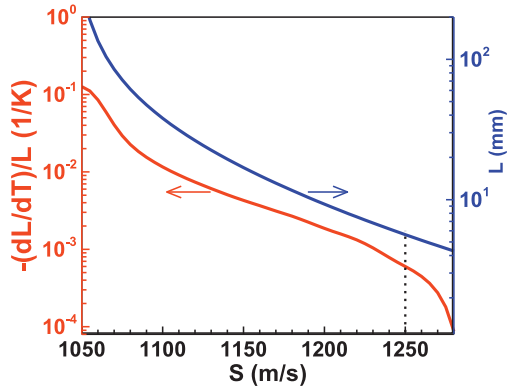

Fig. 11. Chang of the induction length, L, and its relative derivative with respect to pre-shock temperature, $(dL/dt)/L$, with the shock speed.

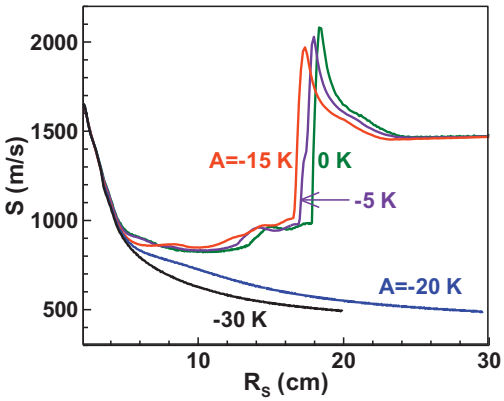

Fig. 10. Shock speed, S, as a function of its position, R_S, for different amplitude of temperature perturbations (A<0, cold spot), with E_S=520 J/m.

detonation initiations. It is seen that for fixed value of E_S=490 J/m, successful detonation initiation is always achieved for a hot spot with A>25 K and it is also achieved for a cold spot with $-16 \le A \le -8$ K. Consistent with results shown in Figs. 6 and 8, Fig. 9 shows that at small amplitude of temperature perturbation, direct denotation initiation is promoted/inhibited by a cold/hot spot. This observation is unexpected and not reported in previous studies. When the amplitude of temperature perturbation is large (i.e., $A<-16$ K or $A>25$ K), as expected, direct denotation initiation is inhibited/promoted by a cold/hot spot.

The above results are obtained for the subcritical case of E_S=490 J/m. Similar observation is also made for the critical case of E_S=520 J/m, for which Fig. 10 shows the influence of a cold spot on the direction detonation initiation. It is observed that a cold spot with small amplitude of temperature perturbation, $-15 \le A < 0$ K, slightly promotes detonation initiation and that it inhibits detonation initiation for $A \le -20$ K. The trend is similar to that shown in Fig. 6 for E_S=490 J/m.

To explain the unexpected observation mentioned above, here we discuss how local low temperature in a cold spot affects detonation initiation. When the shock passes through a cold spot, the influence of the cold spot is twofold: it has both negative and positive effects. The negative effect is that shock speed decreases and so does the post-shock temperature, resulting in lower chemical reaction rate and longer induction length post shock; and thus detonation initiation is inhibited. The positive effect is that a cold spot corresponds to larger local energy density (higher density at lower temperature since the pressure is kept constant, as mentioned in Section 2) and thereby more heat release, which is like adding additional initiation energy and thereby promotes detonation initiation. It is noted that for the case of the cold spot of $A=-10$ K, the increase in the energy contained in the region of $3 \le r \le 4$ cm is within 2% compared to the case without a cold spot. Such small increase can promote direction detonation initiation since the initiation energy (490 J/m in Fig. 6) is close to the critical value.

At small amplitude of temperature perturbation (i.e., small value of $|A|$), the positive effect dominates and a cold spot enhances detonation initiation; and the opposite trend occurs at large amplitude of temperature perturbation. Figure 11 shows the induction length, L, as a function of shock speed. The results are based on the ZND theory and obtained by using the Shock and Detonation Toolbox [28]. We choose the shock speed at R_S=3.5 cm (the center of the region with temperature perturbation) as the characteristic speed when the shock passes through the cold/hot spot. From Fig. 6, the characteristic shock speeds for A=0, $A=-10$ K and $A=-50$ K are 1250 m/s, 1241 m/s

and 1140 m/s, respectively. According to Fig. 11, at these given shock speeds, the corresponding induction lengths are respectively 5.6 mm, 6.1 mm and 19.4 mm. Therefore, the induction length increases dramatically as the amplitude of the cold spot increases from −10 K to −50 K. For A=−10 K, the increase in induction length is 0.5 mm; which for A=−50 K, the increase in induction length is 13.8 mm. This indicates that the intensity of the negative effect increases dramatically with $|A|$. Since the positive effect changes linearly with $|A|$, the positive effect dominates at small value of $|A|$ while the negative effect dominates at large value of $|A|$. This helps to explain the unexpected influence of a cold spot on direct detonation imitation. Figure 11 also shows the sensitivity of induction length to pre-shock temperature, $(dL/dT)/L$. When shock speed decreases from 1250 m/s to 1050 m/s, $(dL/dT)/L$ increases by more than three orders of magnitude. This fact indicates that the negative effect of cold spot increases dramatically as the shock speed decreases. Consequently, the same cold spots located in the quasi-steady region (which has relatively low shock speed) cannot enhance detonation initiation. This is demonstrated by simulation results not shown due to space limit.

It is noted that a cold spot results in the increase of the local density and thereby also increases the local acoustic impedance. Consequently, the shock wave propagation and detonation development are possibly affected by the local change in acoustic impedance, which were studied by Li et al. [29, 30]. According to our simulation, at the moment that the shock passes through the cold spot, the shock speed only slightly changes since the temperature perturbation caused by the cold spot is small.

4. Conclusions

Direct initiation of 1D cylindrical detonation in H_2/O_2/Ar mixture is simulated with detailed chemistry. The emphasis is placed on examining and interpreting the influence of temperature perturbation on direct detonation initiation. First, cases without temperature perturbation are studied. Three regimes, supercritical, critical and subcritical, for direct detonation initiation are identified by decreasing the initiation energy. The quasi-steady period in the critical case is investigated in details. It is found that the abrupt formation of an over-driven detonation after the quasi-steady the period is due to the coherent coupling between pressure pulse and chemical heat release. Then, the effects of cold and hot spots on direct detonation initiation are examined. When the amplitude of temperature perturbation is large enough, a cold/hot spot inhibits/promotes direct denotation initiation. This is expected and similar observation was made in previous studies on hot spot. However, it is observed for the first time that at small amplitude of temperature perturbation, direct denotation initiation is promoted/inhibited by a cold/hot spot. Such unexpected trend is caused by the opposite effects of temperature perturbation: local low temperature reduces the chemical reaction rate while it also increases the local volumetric energy density. At large amplitude of temperature perturbation, the reduction in reaction rate dominates and thereby a cold spot inhibits detonation initiation; while at small amplitude of temperature perturbation, the increase in local volumetric energy density dominates and thus a cold spot promotes detonation initiation.

It is noted that a single cold /hot spot at fixed position is considered in the present study. Our preliminary simulation results indicate that when a different profile of cold/hot spot is used, similar results can be obtained. Besides, the direct detonation initiation depends on the location and number of cold/hot spot. This deserves further study. In realistic flow, the temperature perturbation is much more complicated than the simple 1D case considered in this study. Temperature fluctuations with stochastic distributions are present in realistic flow, which may affect the direction detonation initiation. As suggested by one of the reviewers, this is another topic that deserves further study.

Acknowledgments

This work was supported by National Natural Science Foundation of China (no. 51322602). We appreciate helpful discussions with Hoi Dick Ng at Concordia University, Yiguang Ju at Princeton University and Jianling Li at Northwestern Polytechnical University.

Supplementary materials

Supplementary material associated with this article can be found, in the online version, at doi:10.1016/j.proci.2016.06.093.

References

[1] G.G. Bach, R. Knystautas, J.H. Lee, *Symp. Int. Combust.* 12 (1969) 853–864.
[2] L. He, P. Clavin, *J. Fluid Mech.* 277 (1994) 227–248.
[3] B. Zhang, C. Bai, *Fuel* 117 (2014) 294–308.
[4] L. He, *Combust. Flame* 104 (1996) 401–418.
[5] J.H.S. Lee, A.J. Higgins, *Phil. Trans. R. Soc. London* 357 (1999) 3503–3521.
[6] C.A. Eckett, J.J. Quirk, J.E. Shepherd, *J. Fluid Mech.* 421 (2000) 147–183.
[7] A.R. Kasimov, D.S. Stewart, *Theory of direct initiation of gaseous detonations and comparison with experiment* TAM Report No. 1043, University of Illinois at Urbana-Champaign, 2004.

[8] K. Mazaheri Body, *Mechanism of the onset of detonation in blast initiation* PhD thesis, McGill University, Montreal, Canada, 1997.
[9] H.D. Ng, J.H.S. Lee, *J. Fluid Mech.* 476 (2003) 179–211.
[10] K. Im, S.T. Yu, *AIAA* (2003) 2003–1318.
[11] B. Wang, S.J. Yu, *AIAA* (2004) 2004–0793.
[12] R.S. Chue, J.H. Lee, F. Zhang, *Shock Waves* 5 (1995) 159–167.
[13] G. Taylor, *Proc. R. Soc. London* 201 (1950) 159–174.
[14] L.I. Sedov, M. Friedman, R.E. Street, *Phys. Today* 13 (1960) 50.
[15] Z. Chen, M.P. Burke, Y. Ju, *Proc. Combust. Inst.* 32 (2009) 1253–1260.
[16] Z. Chen, *Combust. Flame* 157 (2010) 2267–2276.
[17] P. Dai, Z. Chen, *Combust. Flame* 162 (2015) 4183–4193.
[18] W. Zhang, Z. Chen, W. Kong, *Combust. Flame* 159 (2012) 151–160.
[19] H. Yu, W. Han, J. Santner, et al., *Combust. Flame* 161 (2014) 2815–2824.
[20] H. Yu, Z. Chen, *Combust. Flame* 162 (2015) 4102–4111.
[21] Z. Chen, *Combust. Flame* 162 (2015) 2442–2453.
[22] M.O. Conaire, H.J. Curran, J.M. Simmie, W.J. Pitz, C.K. Westbrook, *Int. J. Chem. Kinet.* 36 (2004) 603–622.
[23] J.H.S. Lee, R. Knystautas, N. Yoshikawa, *Acta Astronaut.* 5 (1978) 971–982.
[24] J.H.S. Lee, *The detonation phenomenon*, Cambridge University Press, 2008.
[25] J. Melguizo-Gavilanes, L. Bauwens, *Shock Waves* 23 (2013) 221–231.
[26] J. Melguizo-Gavilanes, N. Rezaeyan, M. Lopez-Aoyagi, L. Bauwens, *Shock Waves* 20 (2010) 467–478.
[27] R. Zhou, J. Wang, *Combust. Flame* 159 (2012) 3632–3645.
[28] S. Browne, J. Ziegler, J.E. Shepherd, Numerical Solution Methods for Shock and Detonation Jump Conditions, GALCIT Report FM2006.006, California Institute of Technology (2008).
[29] J. Li, X. Mi, A.J. Higgins, *Proc. Combust. Inst.* 35 (2015) 2025–2032.
[30] J. Li, X. Mi, *J. Phys. Fluids* 27 (2015) 027102.